Journal of Power Sources 255 (2014) 59–64

Contents lists available at ScienceDirect

Journal of Power Sources

journal homepage: www.elsevier.com/locate/jpowsour

Short communication

Effect of ozone on the performance of solid oxide fuel cell with $Sm_{0.5}Sr_{0.5}CoO_3$ cathode

Zhi-Yuan Chen [a], Li-Jun Wang [a,*], Yu-Dong Gong [b], Dan Tang [b], Fu-Shen Li [c], Kuo-Chih Chou [a]

[a] State Key Laboratory of Advanced Metallurgy and School of Metallurgical and Ecological Engineering, University of Science and Technology Beijing, Beijing 100083, China
[b] School of Chemical & Environment Engineering, China University of Mining & Technology, Beijing 100083, China
[c] School of Materials Science and Engineering, University of Science and Technology Beijing, Beijing 100083, China

HIGHLIGHTS

- The power density of the cell has been enhanced by 140% with the introduction of O_3.
- The enhancement is related to the ionization reactions and oxygen adsorption.
- The rate-determining step of the electrochemical reaction does not changed by O_3.
- Oxygen vacancy concentration of SSC could be increased in ozone-contained ambient.
- The Raman spectra of YSZ/SSC cathode were reported.

ARTICLE INFO

Article history:
Received 8 October 2013
Received in revised form
18 December 2013
Accepted 1 January 2014
Available online 8 January 2014

Keywords:
Cathode
Solid oxide fuel cell
Samarium-doped strontium cobaltite
Ozone

ABSTRACT

The electrochemical properties of porous composite cathode consisting of $Sm_{0.5}Sr_{0.5}CoO_3$ (SSC) and 8 mol% Y_2O_3 doped zirconia (YSZ) have been investigated in Ni/YSZ anode-supported single cells at 600 °C under oxygen with/without ozone conditions. The Microscopic features and X-ray powder diffraction patterns of the cathode don't show obvious change before and after the measurement. However, the power density of the cell increases in ozone-contained ambient, which is approximately 140% higher than that in ozone-free ambient in most. The effect of the ozone on the performance of cathode is also examined by impedance spectra and Raman spectra. The results of the impedance spectra indicate that polarization resistance decreases in the ozone-contained ambient compared with that in ozone-free ambient. And the Raman spectra suggest that the physicochemical properties of SSC/YSZ porous cathode are also modified.

1. Introduction

Solid oxide fuel cells (SOFCs) are well known as a new power generation system for their high efficiency in the conversion of chemical energy to electric power. Recently, great attention has been paid to lower the operating temperature of SOFC from around 1000 to below 600 °C, since lower temperature would solve various problems related to the high temperature operation, such as densification of electrodes, crack formation from stress caused by large differences in the thermal expansion coefficients of the cell components. The reduction of operation temperature can be achieved by thinning the electrolyte layer, or by using highly conductive electrolytes. In such condition, cathode would become critical for the fuel cell performance due to its relative higher activation energy in the low operation temperature [1].

Strontium-doped samarium cobaltite $Sm_{1-x}Sr_xCoO_3$ (SSC) is one of the promising cathode materials [2,3], which exhibit relative high ionic conductivities due to a large concentration of oxide vacancies [4]. But the oxygen permeability of perovskite oxides also depends on the rate of oxygen exchange between the cathode materials and gas [5–8]. Kovalevsky et al. [6] proved that the rate of oxygen exchange at oxides/gas interface could be one of the limiting steps of the oxygen transfer through the $Sm_{1-x}Sr_xCoO_3$. Xia et al. [9] pointed out that the rate-determining step of dense SSC

* Corresponding author. Tel.: +86 10 6233 3622; fax: +86 6233 2570.
E-mail address: lijunwang@ustb.edu.cn (L.-J. Wang).

0378-7753/$ – see front matter © 2014 Published by Elsevier B.V.
http://dx.doi.org/10.1016/j.jpowsour.2014.01.004

cathode was to be adsorption–desorption at the surface of the electrode.

However, from the knowledge of the present authors, the effect of ozone on the performance of cathode materials of SOFC is not reported so far, except one from Abazari et al. [10]. They have studied the effect of ozone on the high-temperature electrical properties of nanostructured yttria-doped ceria (YDC). Ozone could be a promising gas to enhance the SOFC performance at low temperature due to its high oxidation potential and high activity. In the present study, the function of ozone applied with 8 mol% Y_2O_3 doped zirconia & $Sm_{0.5}Sr_{0.5}CoO_3$ (YSZ/SSC) cathode was examined at 600 °C.

2. Experimental procedures

YSZ was used as the electrolyte, and the mixture of NiO and YSZ was used as the anode materials of the anode-supported cell. Metal nitrates solution contained Sm^{3+}, Sr^{2+}, Co^{2+} was added dropwise to the porous YSZ cathode matrix. The cell was heated to 450 °C, converting the precursor into fine powder of the SSC stuck on the YSZ matrix. Thickness of the anode, electrolyte and cathode is about 490, 26, and 60 μm, respectively. And the effective area of the cathode was about 0.3 cm^2. The detailed information on the preparing process of the cell was described in Ref. [11].

The schematic of our experimental setup is shown in Fig. 1. As a current collector, Ag lead wires were fired on the surface of the cathode by a small amount of Ag paste at 600 °C. The Ag pasted was painted and fired at 600 °C on the anode to seal it on the opening of the Al_2O_3 tube using the Al_2O_3–Na_2SiO_3 sealant. Then, the cell assembly was placed in a quartz reactor.

Humidified hydrogen (~3 vol% H_2O) was introduced into the Al_2O_3 tube as fuel gas. On the cathode side, mixed gas (O_2, N_2 and/or O_3) was introduced to the quartz reactor, in which O_3 was generated by the custom-designed ozone generator. The input gas was the mixture of dry oxygen and dry nitrogen at 1 atm with a flow rate of 100 ml min^{-1} (STP) during the operation. The ratio of the pure oxygen and nitrogen was controlled by the mass flowmeters (made by Alicat).

Ozone concentration was controlled by the power regulation of the ozone generator. However, degradation rate of ozone became faster with the temperature increasing. Thus the concentration of ozone in the SOFC camber at high temperature was lower than that in the gas outlet of the ozone generator. When dry air introduced into the equipment, the ozone concentration was measured as 0.684 and 0.474 g m^{-3} in the gas inlet and outlet of the cell at 600 °C during the experiments.

Ozone concentration in the exhausted gas was analyzed by titration. Before the titration process, about 2000 ml exhausted gas containing ozone was absorbed by potassium iodide solution (350 ml deionized water mixed with 20 ml 0.20 g ml^{-1} KI solution); then 5 ml H_2SO_4 solution (oil of vitriol:water = 1:5) was added. After that, the solution was titrated by the 0.1000 mol l^{-1} sodium hyposulfite substance. And the concentration of ozone was calculated from the amount of the substance.

Electrochemical characterizations were performed at 600 °C in an oxygen–nitrogen gas mixture with varies oxygen partial pressure: 0.21, 0.60 and 1.00 atm. Characteristics of the cells were compared under ambient including and excluding ozone, respectively. Electrical measurements were performed by the parstat 2273 electrochemistry workstation. The ac impedance spectroscope was carried in the frequency range of 0.100 Hz to 2 MHz and the voltage amplitude was 5 mV. Current–voltage (I–V) characteristics of the cells were measured using linear sweep voltammetry at a sweep rate of 1 mV s^{-1} after the cell maintaining in the certain atmosphere at least 10–20 min.

Microscopic features of the cells were characterized using a scanning electron microscope (SEM, FEI MLA250). In order to investigate the change of the cathode, X-ray diffraction (XRD, TTR III) and Raman spectrum (Horyba LabRAM HR Evolution) were employed. The sample surface is probed with a 532 nm laser which was kept at 2 mW. The specimens used for Raman spectrum detection were treated in various ambient at 600 °C in 2 h without electrochemical test.

3. Results and discussions

Fig. 2 shows the SEM photos on the section of the YSZ/SSC cathodes before and after the testing at ozone contained ambient at 600 °C. The photo of the cathode exposed in the ozone-free ambient is also shown for comparison. It can be seen that the structures of the cathodes were similar in the three conditions.

Fig. 3 shows the XRD patterns of the cathode before and after the exposing in the test ambient at 600 °C, respectively. Ag_2O which was detected in the ozone treated specimen (Fig. 3(b)) shows the strong oxidizing of ozone. However, YSZ and SSC are both detected in the three specimens without other ceramic phases. It is indicated that the phase of the YSZ/SSC cathode was not modified by the ozone. The strong reflection peaks which were presented on the

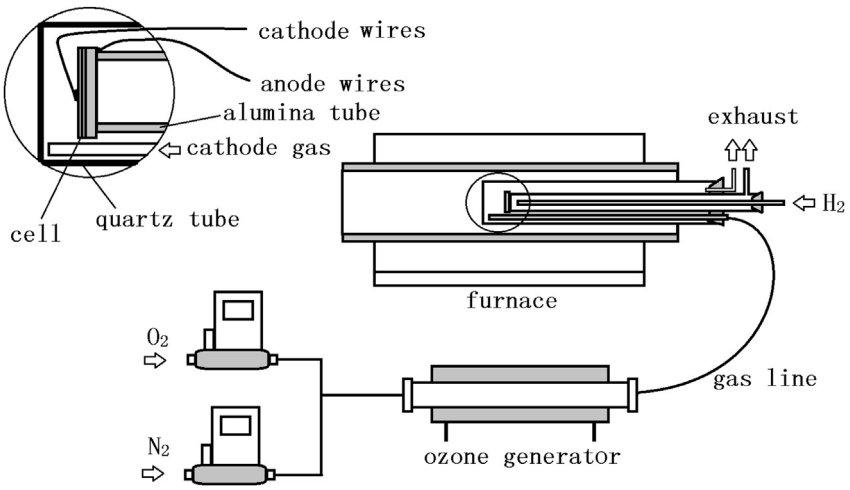

Fig. 1. Schematic of experimental equipments for the electrical measurements of the SOFC.

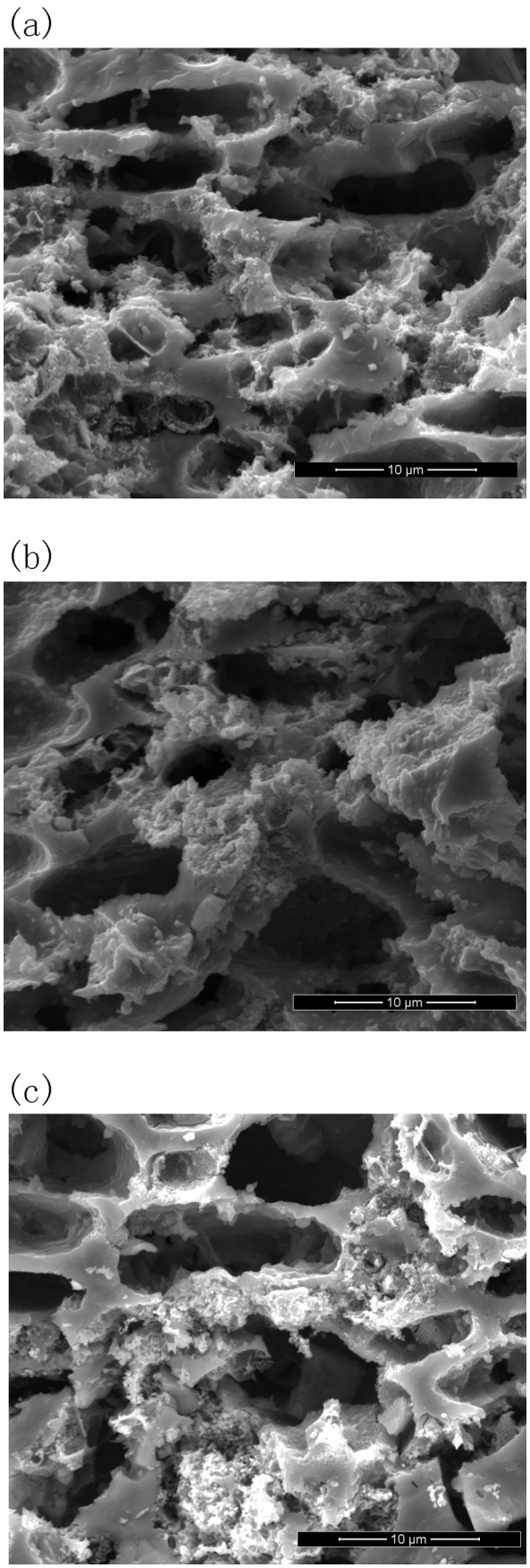

Fig. 2. The SEM photo of the cathode: (a) before the experiment, (b) after exposing in the ozone contained ambient, (c) in the ozone-free ambient at 600 °C.

XRD patterns of YSZ and SSC show a good crystallinity of the cathodic materials.

Fig. 4 shows the dependence of cell voltages and power densities of cell tested at 600 °C in varies atmospheres. It is found that electrochemical properties of the cell were improved significantly in the ozone contained ambient. The maximum power densities of 20, 23 and 23 mW cm^{-2} were obtained from the cell in 21%, 60%, and 100% oxygen-contained atmosphere, respectively. However, these values were much lower than those in the ambient with ozone introduced, which were 25, 43 and 56 mW cm^{-2} in the 21%, 60%, and 100% oxygen contained atmosphere. The maximum power densities increased by 23%, 88%, and 140% correspondingly. It is indicated that introduction of ozone to cathode chamber could enhance output power density of the cell in the present study.

Abazari et al. [10] have assumed that decomposition of ozone on the cathode surface may result in O_3^- and O^-. These new radicals might be benefit to the increase of the power density of the cell. The equilibrium in the oxygen reduction at cathode was suggested to be [12]:

$$O_2\ (\text{gas}) \rightleftharpoons O_2\ (\text{adsorbed}) \rightleftharpoons O_2^- \rightleftharpoons O_2^{2-} \rightleftharpoons O^- \rightleftharpoons O^{2-} \quad (1)$$

Lu et al. [12] observed that the increase of infrared spectroscopy peak height of peroxide ions O_2^{2-} was more sensitive than superoxide ions O_2^- to the oxygen partial pressure. It could be an important reason that the power density of the cell increased with the increasing of oxygen pressure on the cathode side. We surmised that the more posterior oxygen particle in the equilibriums (Eq. (1)) could contribute more effectively to the oxygen reduction. Therefore, additional O^- may decrease the energy of the oxygen reduction reaction. However, this is only based on the assumption; comprehensive works are needed.

The theoretic potentials of the involved reactions were calculated and plotted in Fig. 5. It is noticed that the open circuit voltages (OCVs) of the cell operated in ozone contained ambient are higher than that in pure oxygen ambient, even if the partial pressure of ozone in cathode side is low as 0.0001 atm. Thus, enhance the conversion efficiency of SOFC by feeding ozone is promising in the view of thermodynamics. However, the OCVs of the cells in our experiments were around 1.08–1.09 V, which were not affected obviously by the oxygen potential and the ozone concentration. It is indicated that, the OCV of the cell is not only determined by the partial pressure of the reagents. Wu et al. [13] reported that the saturated oxygen pressure for oxygen adsorption on the SSC surface is near the oxygen partial pressure in air. The weak change of the OCV could be due to the slow oxygen surface exchange at the cathode [6,9] and the difference of catalytic activity of YSZ/SSC cathode to the oxygen and ozone. Even worse, the low operation temperature limited the performance of the cell. It is surmised that, the profit of ozone to the conversion efficiency of SOFC would be more effective if the highly active catalysts were employed.

The impedance spectra provide another way to examine the effect of ozone in the cathodic process. As shown in Fig. 6, it is noticed that there is a significant change in the ozone-contained atmosphere when comparing to the ambient without ozone. In the case of the ozone-free ambient, the spectra don't show obvious changes with oxygen pressure, which indicates that the increasing of oxygen pressure has limited effect on the cathodic process. Conversely, when ozone is introduced to the cathodic chamber, the decrease of absolute value of impedance Z with the introduced ozone could be observed.

In order to analyze the observed spectra, an equivalent circuit [14–16] as in Fig. 6 was used to fit the impedance data which measured in our experiments. In this fit, R is resistance, Q is a constant phase elements with the admittance. L is associated with

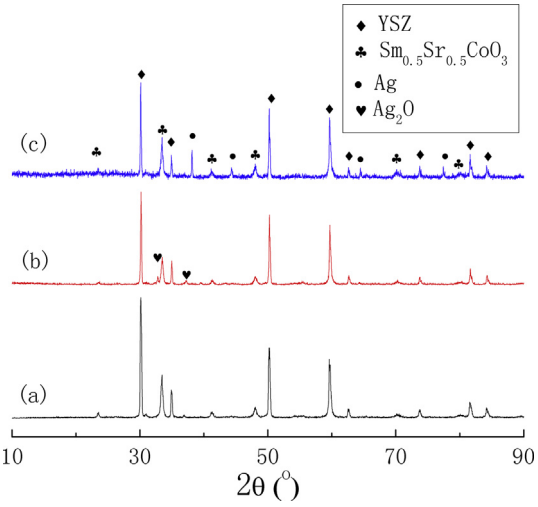

Fig. 3. The XRD spectra of the cathode material: (a) before the experiment, (b) after exposing in the ozone contained ambient, (c) in the ozone-free ambient at 600 °C.

lead inductances, R_s is the electrolyte resistance, R_1 and Q_1 refer to high frequencies, and R_2 and Q_2 correspond to the low frequencies. The parameters n_1 and n_2 indictate the similarity of the Q_1 and Q_2 to a true capacitor, respectively. The resistance parameters were extracted from the fitting results (Table 1). The values of R_s around 10^{-3} to 10^{-5} ohm are much less than those of R_1 and R_2. So the electrolyte resistance can be neglected in the analysis. And the interfacial conductivity was calculated from the resistance R and electrode area A as following [16]:

$$\sigma = (R \cdot A)^{-1} \tag{2}$$

A is equal to 0.3 cm^2 here. Fig. 7 shows that the interfacial conductivity of high-frequency (σ_1) is larger than that of low-frequency (σ_2). The high-frequency and the low-frequency processes are assumed to be the ionization reactions and adsorption–desorption process, respectively [16]. So the latter was the rate determining process no matter that the atmosphere contained ozone or not. As seen from Fig. 7, σ_1 and σ_2 increased when the ozone is introduced, which suggests that the ionization reactions and adsorption–desorption process were both accelerated in zone contained ambient.

Activation energies for the processes are hardly to be calculated based on the impedance plots at different temperature. The problem is that it is difficult to control the reacting ozone in a certain

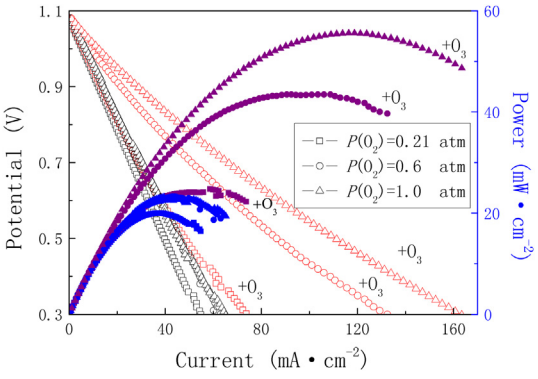

Fig. 4. The I–V curves (open symbols) and the corresponding power densities (solid symbols) at 600 °C for the cell using SSC–YSZ cathode in different atmospheres.

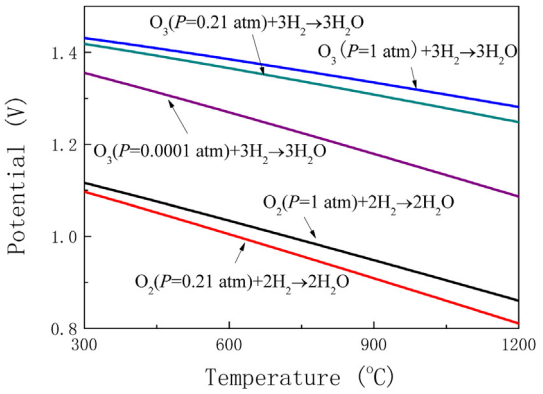

Fig. 5. Theoretical open circuit voltages of the cell working in different ambient.

concentration at different temperature, since the decomposition rate of ozone will increase with the temperature. It is also difficult to quantify the relationship of conductivities of cathode to the ozone concentration for the reason of the uncertainty value of the ozone concentration at high temperature.

The effect of ozone on the YSZ/SSC cathode was characterized by Raman spectra. Fig. 8 shows the spectra of cathode before and after treatment in the ozone-contained ambient (oxygen pressure is around 1 atm). The spectra of the cathode material treated in air and pure oxygen ambient were also detected. The Raman spectra of YSZ have been reported in several references, which the broad band is varied from 530 to 670 cm^{-1} (single F_{2g} mode, which corresponds to the out-of phase motion of the 2 oxygen atoms.) in the Raman

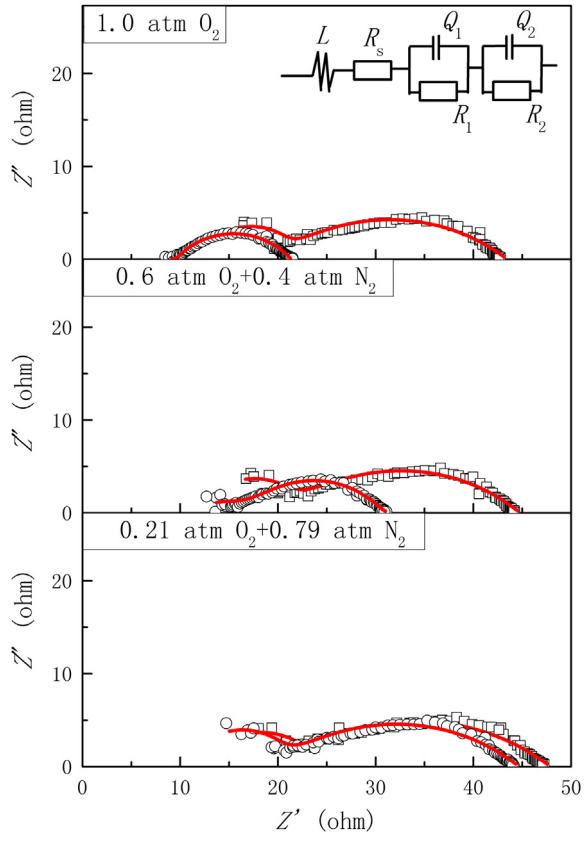

Fig. 6. Impedance plots at 600 °C for the cell with SSC cathode under different ambient.

Table 1
Values of the resistances of the cell in different atmospheres at 600 °C.

$P(O_2)$ (atm)	0.21		0.60		1.00	
	O_3-free	O_3-contained	O_3-free	O_3-contained	O_3-free	O_3-contained
L (H)	1.02×10^{-6}	$4.69E \times 10^{-7}$	4.91×10^{-7}	3.91×10^{-8}	8.00×10^{-7}	$5.29E \times 10^{-7}$
R_s (ohm)	3.98×10^{-3}	1.00×10^{-5}	4.64×10^{-5}	1.00×10^{-4}	1.39×10^{-4}	1.00×10^{-3}
Q_1 (F)	5.36×10^{-9}	2.18×10^{-8}	5.03×10^{-8}	8.79×10^{-4}	4.52×10^{-9}	5.73×10^{-9}
n_1	0.99	0.88	0.83	0.61	0.99	1
R_1 (ohm)	20.3	19.66	20.69	11.45	19.47	9.54
Q_2 (F)	7.95×10^{-4}	9.19×10^{-4}	7.78×10^{-4}	1.21×10^{-3}	8.96×10^{-4}	1.43×10^{-3}
n_2	0.43	0.44	0.46	0.19	0.43	0.55
R_2 (ohm)	27.59	25.02	24.09	20	24.01	11.83

spectra due to the cubic YSZ [17–21]. But the reports about Raman spectra of SSC are rare, except two investigations. One is conducted by Blinn et al. [22], who have studied the surface enhanced Raman spectroscopy of the SSC cathode material. The another one is from Abernathy [23], who detected peaks at 471, 513, and 684 cm^{-1} of dense SSC pellet in the Raman spectrum.

The detected peaks of YSZ matrix (Fig. 8(a)) were the same as Cheng's report [19]. The peaks of the four cathode specimens which are around 620 cm^{-1} are attributed to the YSZ. Weak intensity of this band in the specimens shows that the prod of Raman spectra is limited on the surface of the materials, where the contents of YSZ

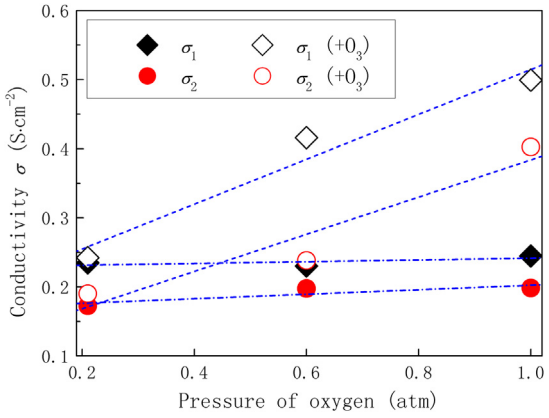

Fig. 7. Interfacial conductivities of the cell in different atmospheres at 600 °C.

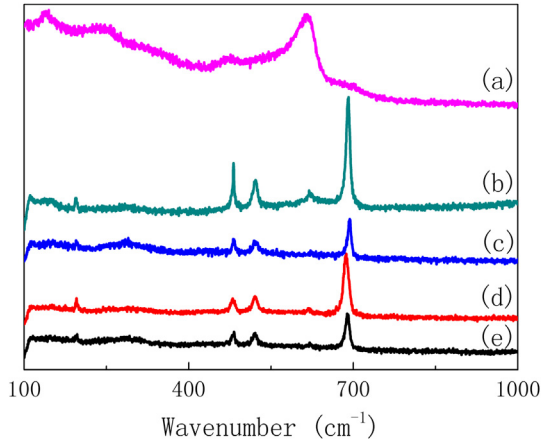

Fig. 8. Raman spectra of (a) YSZ matrix, (b) YSZ/SSC cathode before experiment, (c) YSZ/SSC cathode after exposure to air ambient, (d) YSZ/SSC cathode after exposure to oxygen ambient without ozone, and (e) YSZ/SSC cathode after exposure to oxygen ambient contained ozone at 600 °C for 2 h.

were rare. The other five bands at about 195, 300, 481, 521, and 620 cm^{-1} in Fig. 8(b)–(e) are associated to SSC. The symmetric stretching of the basal oxygen of the octahedral at 620 cm^{-1} (B_{1g} mode) behaves inversely with the mean distances of Co–O bonds in the basal plane [24]. Peaks positions of the observed spectra in this experiment indicate that the cathode material is composited by cubic YSZ and SSC, which is corresponding to the results of XRD spectrum.

The contribution of oxygen vacancy to the Raman spectra has been reported in several forms. The loss in Raman signal intensity of YSZ crystal in the reducing ambient is suggested to be attributed to the increased number of oxygen vacancies [25,26]. And the broader bands of YSZ can be attributed to the structural disorder associated with the oxygen sublattice [18]. The new peak of doped-CeO_2 around 570–600 cm^{-1} is associated with the intrinsic oxygen vacancies, which would increase with the increasing of the oxygen vacancy concentration in the material [27]. The F_{2g} mode was more asymmetric, broader, and band shift to lower frequency when the oxygen vacancies increased [28].

Oxygen vacancy concentration could be less in the cathode when the oxygen partial pressure was raised [13]. As Fig. 8 shows, the B_{1g} mode shows asymmetric with a slight low frequency tail in the spectra expect the symmetric line shape of Fig. 8(d). In additional, intensity of the band increased when the oxygen partial pressure was raised from 0.21 atm to 1.00 atm, but decreased with the ozone introducing. It is suggested that the oxygen vacancy concentration could be more when ozone was fed into the cathode. Moreover, the weakening of Co–O bond could enhance the oxygen surface exchange of Co-based perovskites at high temperature [29,30].

4. Conclusions

The effect of ozone on the electrical properties of SOFC with SSC cathode is investigated at 600 °C. The increased oxygen pressure shows insignificant effect on the power density of the cell. On the contrary, it is found that power densities of the cell in the ozone-contained ambient were 23–140% higher than those in the ozone-free ambient in the current experiment. The OCV of the cell is not visibly changed by the ozone or oxygen partial pressures. As shown in the impedance spectra, the increase in power density of the cell is surmised to be due to the accelerated ionization reactions and adsorption–desorption process in the ozone-contained ambient. The results of XRD and Raman spectra indicate that the compositions of the cathode are still SSC and cubic YSZ after the ozone treatment. But the difference observed in the Raman spectra suggests that ozone could increase the oxygen deficiency concentration of the materials.

Acknowledgments

The authors gratefully acknowledge the financial support of National Program on Key Basic Research Project of China (Grant No.

2012CB215405) and National Nature Science Foundation of China (Nos. 51104013, 51174022). The authors thank Zi-Wei Zheng, Yu-Shuang Niu and Teng-Long Zhu in the China University of Mining & Technology for the material supply and professor Min-Fang Han for her kindness supporting.

References

[1] M. Østergård, C. Clausen, C. Bagger, M. Mogensen, Electrochim. Acta 40 (1995) 1971–1981.
[2] F. Wang, D. Chen, Z. Shao, J. Power Sources 216 (2012) 208–215.
[3] M. Koyama, C.J. Wen, T. Masuyama, J. Otomo, H. Fukunaga, K. Yamada, K. Eguchi, H. Takahashi, J. Electrochem. Soc. 148 (2001) A795–A801.
[4] F. Dong, D. Chen, R. Ran, H. Park, C. Kwak, Z. Shao, Int. J. Hydrogen Energy 37 (2012) 4377–4387.
[5] H. Bouwmeester, H. Kruidhof, A. Burggraaf, Solid State Ionics 72 (1994) 185–194.
[6] A. Kovalevsky, V. Kharton, V. Tikhonovich, E. Naumovich, A. Tonoyan, O. Reut, L. Boginsky, Mater. Sci. Eng. B 52 (1998) 105–116.
[7] S.J. Skinner, J.A. Kilner, Solid State Ionics 135 (2000) 709–712.
[8] S. Kim, Y. Yang, A. Jacobson, B. Abeles, Solid State Ionics 106 (1998) 189–195.
[9] C. Xia, W. Rauch, F. Chen, M. Liu, Solid State Ionics 149 (2002) 11–19.
[10] M. Abazari, M. Tsuchiya, S. Ramanathan, J. Am. Ceram. Soc. 95 (2012) 312–317.
[11] M.F. Han, D. Tang, Z.W. Zheng, Unpublished.
[12] X. Lu, P.W. Faguy, M. Liu, J. Electrochem. Soc. 149 (2002) A1293–A1298.
[13] Q.-H. Wu, H. Abernathy, Z. Cheng, M. Liu, Surf. Rev. Lett. 14 (2007) 587–591.
[14] B. Habibzadeh, University of Maryland, 2007, pp. 103–108.
[15] J. Gao, X. Song, F. Zhou, S. An, Y. Tian, J. Power Sources (2012) 383–392.
[16] H. Fukunaga, M. Koyama, N. Takahashi, C. Wen, K. Yamada, Solid State Ionics 132 (2000) 279–285.
[17] A. Feinberg, C. Perry, J. Phys. Chem. Solids 42 (1981) 513–518.
[18] C. Perry, D.W. Liu, R.P. Ingel, J. Am. Ceram. Soc. 68 (1985) C184–C187.
[19] Z. Cheng, M. Liu, Solid State Ionics 178 (2007) 925–935.
[20] R. Maher, L. Cohen, P. Lohsoontorn, D. Brett, N. Brandon, J. Phys. Chem. A 112 (2008) 1497–1501.
[21] C. Kontoyannis, M. Orkoula, J. Mater. Sci. 29 (1994) 5316–5320.
[22] K.S. Blinn, H.W. Abernathy, M. Liu, in: N.P. Bansal, P. Singh, D. Singh, J. Salem (Eds.), Advances in Solid Oxide Fuel Cells V, John Wiley & Sons, Inc., 2010, pp. 63–73.
[23] H.W. Abernathy III, Georgia Institute of Technology, 2008, pp. 57–58.
[24] W.R. Wang, D.P. Xu, W.H. Su, Z.H. Ding, Y.F. Xue, G.X. Song, Chin. Phys. Lett. 22 (2005) 2400–2402.
[25] M.B. Pomfret, C. Stoltz, B. Varughese, R.A. Walker, Anal. Chem. 77 (2005) 1791–1795.
[26] D. Torres, S. Paje, J. Llopis, G. Morell, R. Katiyar, J. Lumin. 72 (1997) 724–725.
[27] Y. Ji, J. Liu, T. He, J. Wang, W. Su, J. Alloys Compd. 389 (2005) 317–322.
[28] J. McBride, K. Hass, B. Poindexter, W. Weber, J. Appl. Phys. 76 (1994) 2435.
[29] W.T. Hong, M. Gadre, Y.-L. Lee, M.D. Biegalski, H.M. Christen, D. Morgan, Y. Shao-Horn, J. Phys. Chem. Lett. 4 (2013) 2493–2499.
[30] Y.L. Lee, J. Kleis, J. Rossmeisl, Y. Shao-Horn, D. Morgan, Energy Environ. Sci. 4 (2011) 3966–3970.